

## Online Materials<sup>1</sup>.

### 1. Information on Laser–ablation inductively coupled plasma mass spectrometry (LA–ICP–MS) and high-resolution femtosecond laser ablation multi-collector inductively coupled plasma mass spectrometer (fs–LA–MC–ICP–MS) analytical methodologies

LA–ICP–MS analyses were performed in spot mode using a beam diameter of 40  $\mu\text{m}$ , repetition rate of 5 Hz, and laser energy of 4.0 to 5.5 J/cm<sup>2</sup>. Total acquisition time for each analysis was 70 s, with 30 s background measurement followed by 40 s of sample ablation. Calibration for LA–ICP–MS spot analysis was performed using the USGS reference glass NIST SRM-612, using coefficients given by Pearce et al. (1997). Monitored isotopes included <sup>23</sup>Na, <sup>24</sup>Mg, <sup>43</sup>Ca, <sup>55</sup>Mn, <sup>88</sup>Sr, <sup>89</sup>Y, <sup>93</sup>Nb, <sup>95</sup>Mo, <sup>139</sup>La, <sup>140</sup>Ce, <sup>141</sup>Pr, <sup>146</sup>Nd, <sup>147</sup>Sm, <sup>153</sup>Eu, <sup>157</sup>Gd, <sup>159</sup>Tb, <sup>163</sup>Dy, <sup>165</sup>Ho, <sup>166</sup>Er, <sup>169</sup>Tm, <sup>172</sup>Yb, <sup>175</sup>Lu, <sup>182</sup>W, <sup>206</sup>Pb, <sup>207</sup>Pb and <sup>208</sup>Pb. Internal calibration used <sup>44</sup>Ca assuming ideal stoichiometry of scheelite for quantification. Average minimum detection limits and dwell time for all elements are listed in Table S2. Data reduction and processing used Iolite v2.5, a software package for processing LA–ICP–MS data (Paton et al. 2011), as an add-in for the data analysis program Igor (WaveMetrics).

LA–ICP–MS mapping was conducted by ablating sets of parallel lines rastered across an area of the sample using a beam diameter of 9  $\mu\text{m}$  at a laser frequency of 10 Hz. Dwell times for all elements are listed in Table S2. Re-deposition during mapping was minimized by pre-ablating each line prior to data collection. Identical raster lines were performed on standard NIST SRM-612 at the start and end of each mapping run to correct for instrument drift. Element maps were compiled and processed using Iolite data analysis program Igor.

*In-situ* Sr and Nd isotope measurements by fs–LA–MC–ICP–MS were performed on a Neptune Plus MC–ICP–MS (Thermo Fisher Scientific, Germany) in combination with a J-200 343 nm femtosecond (fs) laser ablation system (Applied Spectra, USA) housed at the National Research Center for Geoanalysis, Chinese Academy of Geological Sciences (CAGS), Beijing, China. The JET sample and X skimmer cones were used along with the guard electrode (GE), and all measurements were conducted in low-resolution and static modes. Nitrogen (7 ml/min) was added from the sample cell during measurement to increase sensitivity and a buffer-smoothing device was used before ICP to reduce the fluctuation effect induced by laser-ablation pulses (C. Li et al. 2018). At the start of each analytical session, the fs–LA–MC–ICP–MS system was optimized using NIST 612 to achieve maximum signal intensity and low oxide rates. Samples were ablated in line mode with spot size of 40  $\mu\text{m}$ , line length of 20  $\mu\text{m}$ , stage movement speed of 0.65  $\mu\text{m/s}$ , laser repetition rate of 8 Hz, and beam energy density of 10 J/cm<sup>2</sup>. An integration time of 15 s was used for acquisition of the background signal prior to ablation, followed by a 32 s sample signal with an integration time of 0.262 s. For Sr isotope analyses, outliers were rejected based on a 2 $\sigma$  criterion for all data with <sup>88</sup>Sr intensity >0.35 voltage (C. Li et al. 2018). The instrumental mass bias for Sr isotopes was corrected using an exponential law function based on <sup>86</sup>Sr/<sup>88</sup>Sr value of 0.1194. In-house scheelite reference materials HTPW and XJSW (C. Li et al. 2018) were analyzed every 10 samples. The instrumental mass bias for Nd and Sm isotopes was corrected using an exponential law function based on a <sup>146</sup>Nd/<sup>144</sup>Nd value of 0.7219 and <sup>147</sup>Sm/<sup>149</sup>Sm value of 1.0868 (Yang et al. 2014). Interference of <sup>143</sup>Sm on <sup>143</sup>Nd was corrected based on the measured signal intensities of <sup>147</sup>Sm, mass bias coefficient and the natural isotopic composition. An in-house scheelite reference material (XWC) and Durango apatite (Foster and Vance 2006; Yang et al. 2014) were analysed after every 10 samples to monitor instrument stability and allow external correction of <sup>147</sup>Sm/<sup>144</sup>Nd ratios. The analytical uncertainty

for Sr and Nd are generally 500 ppm and 75 ppm when 100  $\mu\text{g}$  sample was ablated and analyzed. Note that the analytical uncertainty is based on their concentrations.

## References cited

- Foster, G.L., and Vance, D. (2006) In situ Nd isotopic analysis of geological materials by laser ablation MC-ICP-MS. *Journal of Analytical Atomic Spectrometry*, 21, 288–296.
- Li, C., Zhou, L.M., Zhao, Z., Zhang, Z.Y., Zhao, H., Li, X.W., and Qu, W.J. (2018) In-situ Sr isotopic measurement of scheelite using fs-LA-MC-ICPMS. *Journal of Asian Earth Sciences*, 160, 38–47.
- Paton, C., Hellstrom, J., Paul, B., Woodhead, J., and Hergt, J. (2011) Iolite: Freeware for the visualisation and processing of mass spectrometric data. *Journal of Analytical Atomic Spectrometry*, 26, 2508–2518.
- Pearce, N.J.G., Perkins, W.T., Westgate, J.A., Gorton, M.P., Jackson, S.E., Neal, C.R., and Chenery, S.P. (1997) A compilation of new and published major and trace element data for NIST SRM 610 and NIST SRM 612 glass reference material. *Geostandards Newsletter*, 21, 115–144.
- Yang, Y.H., Wu, F.Y., Yang, J.H., Chew, D.M., Xie, L.W., Chu, Z.Y., Zhang Y.B., and Huang, C. (2014) Sr and Nd isotopic compositions of apatite reference materials used in U-Th-Pb geochronology. *Chemical Geology*, 385, 35–55.

## 2. Supplemental figures

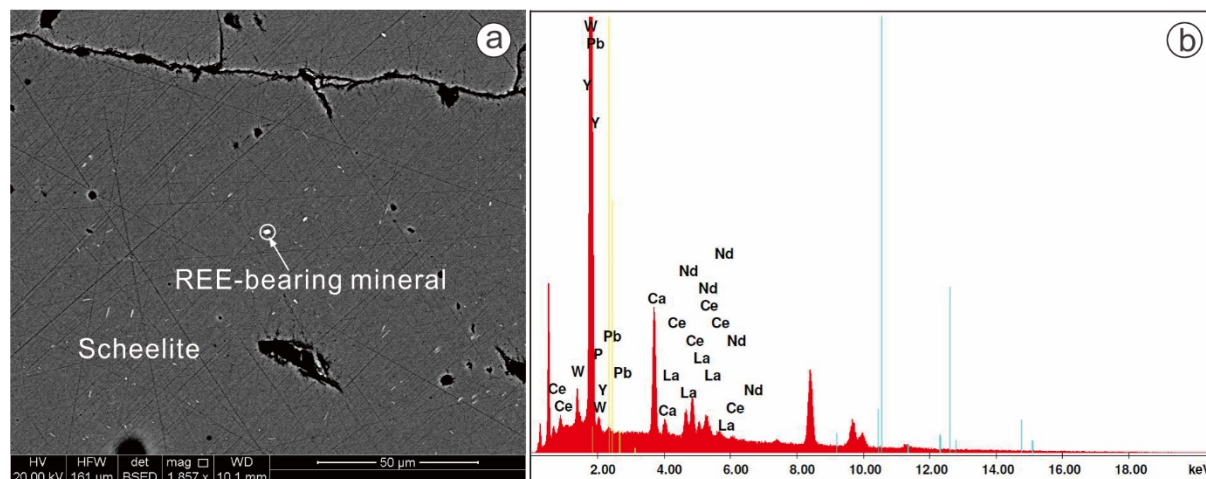


FIGURE OM1. REE-bearing minerals within scheelite. (a) Backscatter electron (BSE) image showing the occurrence of these REE-bearing minerals. (b) Energy dispersive X-ray spectra showing major elements within the REE-bearing minerals

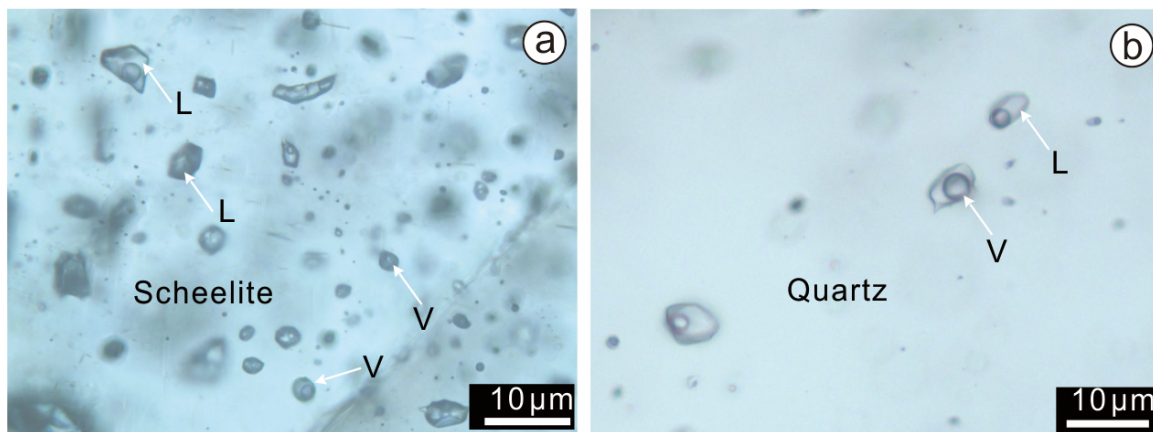


FIGURE OM2. Vapor-rich and liquid-rich fluid inclusions co-existed within scheelite and quartz from Stage 2

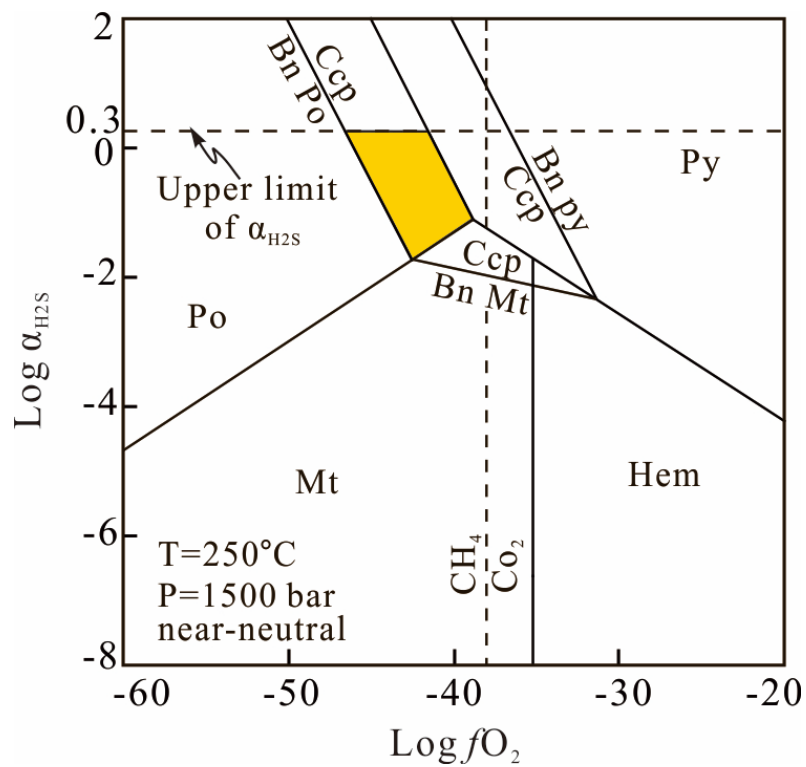


FIGURE OM3. Log  $\alpha_{\text{H}_2\text{S}}$  versus log  $f\text{O}_2$  diagrams showing the fields of stability for sulfides. Minerals include pyrite (Py), Chalcopyrite (Ccp), Pyrrhotite (Po), bornite (Bn), magnetite (Mt), and hematite (Hem).